Near infrared (NIR) spectroscopic evaluation of articular cartilage: A review of current and future trends

3 authors, including:

Ismail Olumegbon
Elizade University
3 PUBLICATIONS   **8** CITATIONS

SEE PROFILE

Isaac Afara
University of Eastern Finland
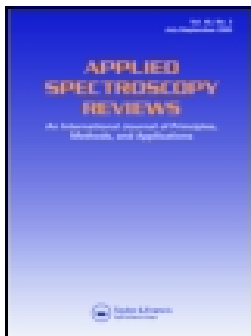**57** PUBLICATIONS   **377** CITATIONS

SEE PROFILE

Some of the authors of this publication are also working on these related projects:

Optical characterization of articular cartilage View project

NIR characterization of Osteochondral tissue View project

Near-infrared (NIR) spectroscopic evaluation of articular cartilage: A review of current and future trends

Ismail Adewale Olumegbon, Adekunle Oloyede & Isaac Oluwaseun Afara

Accepted author version posted online: 20 Oct 2016.
Published online: 20 Oct 2016.

Submit your article to this journal ☑

Article views: 75

View related articles ☑

View Crossmark data ☑

Taylor & Francis
Taylor & Francis Group

Near-infrared (NIR) spectroscopic evaluation of articular cartilage: A review of current and future trends

Ismail Adewale Olumegbon[a], Adekunle Oloyede[b,c], and Isaac Oluwaseun Afara[b,d,e]

[a]Department of Physical and Chemical Science, Elizade University, Ilara-Mokin, Ondo State, Nigeria; [b]Research and Innovation Centre, Elizade University, Ilara-Mokin, Ondo State, Nigeria; [c]School of Chemistry, Physics, and Mechanical Engineering, Institute of Health and Biomedical Innovation, Queensland University of Technology, Brisbane, Queensland, Australia; [d]Department of Electrical & Computer Engineering, Elizade University, Ilara-Mokin, Ondo State, Nigeria; [e]Department of Applied Physics, University of Eastern Finland, Kuopio, Finland

ABSTRACT

This review describes recent developments and applications of near-infrared (NIR) spectroscopy for characterization of articular cartilage integrity. It summarizes the research findings in this area and presents some spectral ranges and peaks associated with the different properties and components of articular cartilage. We further describe recent adaptations of NIR spectroscopy for clinical evaluation of articular cartilage injury and degeneration. Critical to accurate decision-making during repair surgery is having clear knowledge of lesion severity and spread, and how to grade the quality of surrounding cartilage. Thus, in this review, we detail efforts aimed at quantification and classification of cartilage pathology using NIR spectroscopy. Finally, we present open questions and challenges with a view to guiding future directions in NIR spectroscopy research on articular cartilage.

Introduction

Articular cartilage is a specialized connective tissue covering the ends of diarthrodial joints, enabling friction-free movement of articulating joints, as well as transmitting physiological loads to the underlying bone. This tissue is avascular (no blood supply) and aneural (no nerve endings) (1), thus its capacity to heal after injury is limited (2). It is composed of a solid extra-cellular matrix (ECM) (3), consisting of collagen fibril network (10–15%) (4), which forms the framework of the tissue, and ground substance rich in proteoglycans (PG) (5–10%) (5), surrounded by water and mobile ions (60–80%) (6). Structurally, articular cartilage possesses a depth-wise layered architecture, where the composition and structure, collagen fibre orientation, amount of PG, and ion concentration of the tissue depend on the layers (7).

Alteration of the composition and/or structure of articular cartilage, either as a result of injury or aging, often results in degeneration of the tissue and in some cases progression to

---

osteoarthritis (OA), which is the major disease of articular cartilage. Although the pathogenesis of OA is not well understood, its onset is often characterized by biochemical, biomechanical, and morphological changes in articular cartilage (8–10). These changes involve breakdown of cartilage ECM, with associated increase in the tissue water content, resulting in alteration and imbalance of the ECM components (6, 10–16). Thus, clinical assessment of early-stage cartilage pathology is essential in preventing progressive degeneration and development of OA.

Clinical diagnosis of cartilage pathology is often performed by clinical examination and radiography (17–20), in some cases magnetic resonance imaging (MRI) (21–25) may be conducted. Conventional radiography provides indirect diagnosis of OA via joint-space narrowing, and is only sensitive to late or advanced stages of OA (26). MRI's multiplanar capability and superior tissue contrast make it an ideal modality for clinical assessment of cartilage injury and degeneration. Nevertheless, the poor resolution and lack of availability of clinical MRI pose a limitation on the use of this modality for cartilage assessment (27, 28). More so, extraction of tissue biopsies (29–31) from affected joint is unsuitable as it cannot provide real-time assessment during arthroscopic surgery, and it exposes the joint to further degeneration. For confirmation of diagnosis and surgical repair of cartilage injuries and degeneration, arthroscopy is performed. Although minimally invasive and enables access to the joint space for visual examination of the cartilage surface, arthroscopy is a visually subjective and has poor inter- and intra-observer reliability (32–38).

To address these limitations of conventional and existing diagnostic methods, several non-destructive techniques that can provide objective and quantitative evaluation of articular cartilage integrity in real-time, and potentially enhance the outcome of conventional arthroscopy have been proposed and are currently being researched. The proposed non-destructive techniques include NIR spectroscopy (39, 40), Raman spectroscopy (41, 42), optical coherence tomography (OCT) (43–46), Fourier transform infrared spectroscopy (FTIR) (12, 47–53), and high-frequency ultrasound (54–56), with near-infrared (NIR) spectroscopy being one of the most promising of these techniques.

NIR spectroscopy was discovered in 1800 by F.W. Herschel (57), and was first applied in agricultural research (58), where significant development of the techniques was undertaken. In recent years, NIR has been adapted for various applications in biomedical engineering, including analysis of the composition of oxy-haemoglobin (59, 60), lipids (61), water (62), and proteins (63, 64) in body tissues, blood, and urine. In addition, normal and cancerous breast (65) and prostate (66) tissues can be differentiated using this technique. Furthermore, measurement of blood glucose level has also been demonstrated using NIR (67–69). Although NIR spectroscopy has been employed in the study of synovial fluid for diagnosis of arthritis (70), its application for evaluation and characterization of articular cartilage integrity is fairly recent. It enables non-destructive spectroscopic probing of cartilage matrix in order monitor changes in the tissue and provides insight into the structure–function relationship in early OA, as well as assist decision making during arthroscopic surgery. This review focuses on the application of NIR spectroscopy for characterization of articular cartilage properties, with particular emphasis on the specific spectral regions employed by researchers for characterizing the different properties and function of articular cartilage.

Fundamentals of NIR spectroscopy

NIR spectroscopy is a vibrational spectroscopic technique, between the spectral range 800 nm and 2,500 nm (71, 72), that produces complex absorption peaks resulting from overtones of fundamental absorption peaks in the infrared spectral range (2,500–20,000 nm) (73). Absorption in the NIR spectral range originates from overtones and combinations of stretching and bending vibrations of O—H, C—H, N—H, and S—H bonds (74, 75), which are the major molecular bonds in organic materials. The peaks in NIR spectroscopy tend to be broad and overlapping; thus, this technique is non-specific and relies on chemometrics and multivariate analyses to extract hidden/latent information from the spectra of materials. NIR spectroscopy is based on the ability of materials to absorb and scatter NIR light at different wavelengths.

The behavior of molecules under NIR excitation can be modeled by an anharmonic oscillator with energy of vibration given by

$$E_{vib} = h\nu[1 - (2\nu + \Delta\nu + 1)y], \tag{1}$$

where E_{vib} is the vibrational energy, h is the Planck constant, ν is the frequency of vibration, $\Delta\nu$ is the vibrational energy states ($\Delta\nu = \pm 2, \pm 3\ldots$), and y is the anharmonic factor.

This anharmonicity introduces overtones (integral multiples of fundamental absorption frequencies) and combination bands into the energy system. These overtone and combination bands are peculiar to NIR and are 10–100 times weaker relative to the fundamental frequencies in the IR spectral region (76). The peaks in NIR originate from the X–H stretching and bending modes (X=S, N, O, C), which is the bonding of hydrogen to other light atoms. The matrix components of articular cartilage (collagen and PGs) are mainly composed of macromolecules-containing bonds that are sensitive to NIR probing (CH, OH, NH, SH). This makes NIR spectroscopy a suitable optical technique for probing molecular, micro-, and macroscopic changes in articular cartilage.

Unlike other optical techniques, viz. Raman spectroscopy, OCT, and FTIR spectroscopy, NIR is an ideal optical spectroscopic tool of choice for probing of articular cartilage integrity because of its relatively high penetration depth into organic materials (77–80), which depends on the spectral wavelength, sample features, and NIR light intensity. The ability of NIR light to penetrate deep into biological tissues, up to about 8.5 mm into neonatal head (80), is an inherent advantage it possess over other spectroscopic techniques, especially in probing full-thickness cartilage, and potentially subchondral bone properties (81) (articular cartilage thickness in the human joint ranges from 1 mm to 4 mm). In addition, the technique requires no sample preparation, making it ideal for *in vivo* assessment of cartilage integrity.

Trend of NIR research on articular cartilage

Research into application of NIR spectroscopy for evaluation of cartilage integrity is as recent as a decade, when Spahn et al. demonstrated NIR spectroscopy as a potential method for arthroscopic evaluation of low-grade degenerated cartilage lesions (40). Table 1 highlights, in chronological order, the literature on the capacity and application

Table 1. A systematic and chronological literature review of the application of NIR spectroscopy for evaluation of articular cartilage.

S/N	Author(s)	Specimen and methodology	Spectral region, wavenumber (cm^{-1})	Type of study	Results
1	Spahn et al., 2007 (40)	Patients ($N = 12$) suffering from knee pain for over 3 months	5,882–9,091	C	NIRS has a significantly ($p = .000$) higher specificity (0.96) and accuracy (0.98) than MRI (0.54 and 0.70, respectively).
2	Spahn et al., 2008 (72)	Sheep knees ($N = 22$)	5,882–9,091	E	Correlation between NIRS absorption and water content ($R = 0.804$), histological Mankin Score ($R = 0.605$), and reduced stiffness via Shore A parameter ($R = 0.695$).
3	Brown et al., 2009 (82)	Bovine patella ($N = 6$). Experimental chondropathy by Trypsin digestion	4,000–12,500	E	Significant decrease of NIRS-absorption within specimens after digestion).
4	Spahn et al., 2010 (83)	Patients ($N = 15$) undergoing arthroscopic knee operations	5,882–11,111	C	NIRS shows a significant ($p < .001$) correlation within the observers of $R = 0.885 \pm 0.036$.
5	Hofmann et al., 2010 (84)	Patients ($N = 21$) with knee pain lasting for half a year	6,780–8,696	C	Significant ($p > .007$) correlations with three KOOS sub-scores only were found with NIRS. The Spearman's rank correlation coefficient ranged between 0.68 and 0.72.
6	Baykal et al., 2010 (85)	Engineered cartilage constructs (Collagen-I Scaffolds)	3,800–5,400	E	Significant correlation between NIRS-absorption and cartilage collagen content ($R = 0.93$, $p < .0001$), and PG content ($R = 0.79$, $p < .0001$).
7	Marticke et al., 2010 (86)	Human cartilage-bone specimens ($N = 200$; 4 mm diameter plugs)	5,882–9,091	C	Significant correlation between NIRS-absorption and ICRS grade ($R = 0.467$) and Young's Modulus ($R = 0.535$).
8	Brown et al., 2011 (87)	Bovine patella, normal cartilage ($N = 10$), and cartilage lesions in different ICRS-grades ($N = 10$)	4,250–11,000	E	Distinction between normal cartilage lesions (accuracy 95%). Poor correlation between NIRS-measurement and cartilage histology ($R = 0.410$) or reduced content of PG ($R = 0.220$).
9	Johansson et al., 2011 (88)	Samples ($N = 9$) from patients undergoing knee replacement surgeries	9,091–50,000	E	NIRS shows high correlation coefficient after normalization to red region ($R = 0.86$) and for the green region ($R = 0.80$).
10	Brown et al., 2012 (89)	Bovine patella, normal cartilage ($N = 10$), and cartilage lesions in different ICRS-grades ($N = 10$)	4,000–12,500	E	The ultrasound reflection coefficient correlates with the mechanical parameters ($r > 0.5$). The DR-NIRS parameters correlate with the ultrasound reflection parameters (r; 0.8 for surface reflection).
11	Hoffmann et al., 2012 (90)	Scaffold-free tissue engineered cartilage constructs	6,061–10,526	E	The change of absorption at absorption maximum (1,453 nm) is positive for intact cartilage and negative for degenerative cartilage.
12	Afara et al., 2012 (74)	Three different OA models in rats ($N = 36$)	9,967–12,436	E	Correlation ($R^2 = 95.89\%$, $p < .0001$) between NIRS absorption and grade of cartilage destruction based on Mankin histological score.
13	Afara et al., 2013 (39)	Bovine patella ($N = 15$, $N = 97$)	5,350–8,850	E	High linear correlation ($R^2 = 93.89\%$, $p < .0001$) between NIR absorption spectra and articular cartilage thickness.
14	Afara et al., 2013 (79)	Bovine patella ($N = 13$)	Combination of 5,700–6,100 and 7,500–12,500	E	Significant correlation ($R^2 = 95.89\%$, $p < .0001$) between spectral data and biomechanical/recovery characteristic of articular cartilage.
15	Afara et al., 2013 (91)	Bovine patella ($N = 15$)	4,000–12,500	E	Significant correlation between NIRS absorption spectra and cartilage thickness ($R^2 = 93.02\%$, $p < .0001$), stress ($65.46\% \leq R^2 \leq 66.04\%$, $p < .0001$).

#	Reference	Sample	Spectral range	Type	Findings
16	Spahn et al., 2013 (92)	Patients with degenerative knee ($N = 6$) versus traumatic knee ($N = 6$)	5,882–11,111	C	The mean NIR absorption value of 71.5 was obtained for traumatic knee, and 31.7 for degenerative knee.
17	Padalkar et al., 2013 (93)	Bovine nasal cartilage ($N = 2$)	5,200–6,890	E	Integrated areas of both absorbance bands correlate linearly with the absolute water content ($R = 0.87$ and 0.86) and with percent water content ($R = 0.97$ and 0.96) of the tissue.
18	Guenther et al., 2014 (94)	Miniature pigs osteochondral samples ($N = 10$)	5,882–11,111	E	In the central area, NIRS measurement shows low correlation ($R = -0.379$, $R = -0.182$, $p < .05$) with histological scores.
19	McGoverin et al., 2014 (95)	Bovine bone and cartilage from human tibial plateaus ($N = 22$)	4,000–12,000	E	Significant linear correlation between NIRS absorption spectra and Cartilage thickness ($R^2 = 0.61$), modified Mankin grade ($R^2 = 0.64$).
20	Palukuru et al., 2014 (96)	Bovine type II collagen, bovine cartilage derived chondroitin sulfate powder, and bovine knee joints and snouts	4,000–5,000	E	Significant correlation between NIRS and collagen and chondroitin sulphate (PG) content ($R^2 = 0.95$, and RMSEP 8% w/dw).
21	Afara et al., 2014 (97)	Three different OA models in rats ($N = 36$)	Combined spectral range: 5,446–6,113; 7,500–10,500; and 9,967–12,436	E	Significant correlation between NIRS absorption spectra and structural integrity ($R^2 = 94.78\%$, $p < .0001$), cellularity ($R^2 = 88.03\%$, $p < .0001$), and staining score ($R^2 = 96.39\%$, $p < .0001$).
22	Afara et al., 2014 (98)	Bovine patella ($N = 6$, $N = 20$)	Combination of 5,440–6,540 and 9,959–12,489	E	Significant correlation ($R^2 = 91.40\%$, $p < .0001$) between NIR spectral data and PG content, and spatial mapping of PG content in articular cartilage.
23	Afara et al., 2015 (44)	Human cadaver knees ($N = 13$, $N = 50$)	9,091–10,309	E	Significant correlation between NIR absorption spectra and biomechanical properties ($60.8\% \le R^2 \le 72.0\%$, $p < .0001$), biochemical properties ($77.3\% \le R^2 \le 78.0\%$, $p < .0001$), and histological properties ($65.0\% \le R^2 \le 77.9\%$, $p < .0001$).
24	Padalkar et al., 2015 (99)	Bovine knee joints ($N = 5$)	4,000–10,000	E	The depth of penetration varied from ~1 mm to 2 mm in the 4,000–5,100 cm^{-1} range, ~3 mm in the 5,100–7,000 cm^{-1} range, and ~5 mm in the 7,000–9,000 cm^{-1} spectral range.
25	McGoverin et al., 2016 (100)	Engineered cartilage constructs (bovine joints)	4,000–10,000	E	Significant correlation between spectral data and water content ($R = 0.68$, $p = .03$), PG content ($R = 0.82$, $p = .007$), and collagen content ($R = 0.84$, $p = .005$).
26	Palukuru et al., 2106 (101)	Bovine knee joints and nasal snouts	4,000–6,000	E	NIR spectra predicted the MIR-determined values of PG/Collagen within 6% of actual values.
27	Sarin et al., 2016 (102)	Equine joints ($N = 44$)	4,000–27,778	E	Significant correlation between spectral data and cartilage thickness ($R^2 = 70.3\%$, $p < .0001$), equilibrium modulus ($R^2 = 67.8\%$, $p < .0001$), Dynamic modulus ($R^2 = 68.9\%$, $p < .0001$), and instantaneous modulus ($R^2 = 41.8\%$, $p < .0001$).
28	Afara et al., 2016 (103)	Bovine patellae ($N = 12$)	12,500–4,000	E	Significant linear correlation between NIRS absorption spectra and elastic rebound ($R^2 = 98.35\%$, $p < .0001$).

Notes: Study type: E = experimental; C = clinical.
Only studies that have used spectral data within the IUPAC defined wavenumber region are considered: 4,000–12,500 cm^{-1} = 2,500–800 nm.

of NIR for characterization of articular cartilage injury, defects, and integrity in both human and animal joints.

NIR spectroscopic characterization of articular cartilage properties

Due to the capacity of NIR spectroscopy to monitor key chemical (104, 105), physical (106, 107), and functional (108) properties of biological materials, the technique has been adopted for assessing changes in the functional, biochemical, and structural properties of articular cartilage. Highlighted below are studies that have demonstrated the capability of NIR spectroscopy for assessment of the functional (Table 2), biochemical (Table 3), and structural (Table 4) properties of articular cartilage.

Peak assignments of articular cartilage NIR spectra

The ability of NIR spectroscopy to track important physio-chemical and morphological changes in organic materials makes it a suitable technique for monitoring biochemical changes in articular cartilage, which has been shown to be related to its biomechanical and functional properties due to the structure–function relationship of the tissue. Hence, the NIR spectrum of articular cartilage incorporates latent information on its physical, morphological, and functional properties. Thus, accurate peak definitions, which are associated with the biochemical composition of articular cartilage, can have significant influence on the reliability of spectral interpretation and analyses with regards to characterization of the tissue properties. This review presents a list of common spectral regions in the NIR spectra of osteochondral tissue (Figure 1), and the associated molecular assignment related to the matrix components of the tissue (Table 5).

Table 2. Systematic review of the application of NIR spectroscopy for evaluation of articular cartilage functional properties.

S/N	Author(s)	Spectral region, wavenumber (cm^{-1})	Specimen	Functional property	NIR correlation
1	Spahn et al., 2008 (72)	5,882–9,091	Ovine medial femoral condyle ($N = 22$)	Mechanical stiffness	$R = 0.877$
2	Marticke et al., 2010 (86)	5,882–9,091	Human knee ($N = 200$)	Young modulus	$p = 0.535$
3	Afara et al., 2013 (79)	12,500–7500, 6100–5700	Bovine patellae ($N = 13$)	Osmotic reswelling	$R^2 = 95.89\%$
4	Afara et al., 2013 (91)	4000–12500	Bovine patellae ($N = 15$)	Stress	$65.46\% \leq R^2 \leq 66.04\%$
5	Afara et al., 2015 (44)	9,091–10,309	Human cadaver knees ($N = 13, N = 50$)	Dynamic modulus	$R^2 = 72.0\%$
6	Afara et al., 2015 (44)	9,091–10,309	Human cadaver knees ($N = 13, N = 50$)	Equilibrium modulus	$R^2 = 60.8\%$
7	Afara et al., 2016 (103)	5,450–6,100, 7,500–12,500	Bovine patellae ($N = 12$)	Elastic rebound	$R^2 = 98.35\%$
8	Brown et al., 2012 (89)	4,000–12,500	Bovine patella, normal cartilage ($N = 10$), and cartilage lesions in different ICRS-grades ($N = 10$)	Structural electric parameter (SEP)	$R = 0.55$
9	Sarin et al., 2016 (102)	9,524–14,286	Equine joints ($N = 44$)	Equilibrium modulus	$R^2 = 67.8\%$
10	Sarin et al., 2016 (102)	9,524–14,286	Equine joints ($N = 44$)	Dynamic modulus	$R^2 = 68.9\%$
11	Sarin et al., 2016 (102)	9,524–14,286	Equine joints ($N = 44$)	Instantaneous modulus	$R^2 = 41.8\%$

Table 3. Systematic review of the application of NIR spectroscopy for evaluation of articular cartilage biochemical properties.

S/N	Author(s)	Spectral region, wavenumber (cm^{-1})	Specimen	Biochemical property	NIR correlation
1	Afara et al., 2015 (44)	9,091–10,309	Human cadaver knees ($N = 13$, $N = 50$)	Water content	$R^2 = 65.0\%$
2	Afara et al., 2015 (44)	9,091–10,309	Human cadaver knees ($N = 13$, $N = 50$)	Uronic acid (indicative of PG content)	$R^2 = 77.9\%$
3	Spahn et al., 2008 (72)	5,882–9,091	Ovine medial femoral condyle ($N = 22$)	Water content	$R = 0.845$
4	Padalkar et al., 2013 (93)	5200–6890	Bovine nasal cartilage ($N = 2$)	Water content	$R = 0.87$
5	McGoverin et al., 2016 (100)	4,000–10,000	Engineered cartilage constructs (bovine joints)	Water content	$R = 0.68$
6	McGoverin et al., 2016 (100)	4,000–10,000	Engineered cartilage constructs (bovinejoints)	PG content	$R = 0.82$
7	McGoverin et al., 2016 (100)	4,000–10,000	Engineered cartilage constructs (bovine joints)	Collagen content	$R = 0.84$
8	Palukuru et al., 2106 (101)	4,000–6,000	Bovine knee joints and nasal snouts	PG/Collagen content	RMSEP = 6%

Table 4. Systematic review of the application of NIR spectroscopy for evaluation of articular cartilage structural (histological and thickness) properties.

| S/N	Authors(s)	Spectral region, wavenumber (cm^{-1})	Specimen	Structural property	NIR correlation
1	Afara et al., 2015 (44)	9,091–10,309	Human cadaver knees ($N = 13$, $N = 50$)	Mankin score	$R^2 = 77.3\%$
2	Afara et al., 2015 (44)	9,091–10,309	Human cadaver knees ($N = 13$, $N = 50$)	Thickness	$R^2 = 78\%$
3	Spahn et al., 2008 (72)	5,882–9,091	Ovine medial femoral condyle ($N = 22$)	Mankin score	$R = 0.896$
4	Afara et al., 2013 (39)	5,350–8,850	Bovine patella ($N = 15$)	Thickness	$R^2 = 93.1\%$
5	McGoverin et al., 2014 (95)	7,280–6,040 and 8,820–8,060	Bovine bone and cartilage, human tibial plateaus ($N = 22$)	Thickness	$R^2 = 75\%$ $R = 0.61$
6	McGoverin et al., 2014 (95)	7,460–6,780 and 8,695–8,197	Bovine bone and cartilage, human tibial plateaus ($N = 22$)	Modified Mankin score	$R^2 = 84\%$ $R = 0.6$
7	Guenther et al., 2014 (94)	5,882–11,111	Miniature pigs osteochondral samples ($N = 10$)	Wakitani score	$R = -0.379$
8	Guenther et al., 2014 (94)	5,882–11,111	Miniature pigs osteochondral samples ($N = 10$)	Pineda score	$R = -0.182$
9	Afara et al., 2012 (74)	12,436–9,967	OA models in rats ($N = 36$)	Mankin score	$R^2 = 88.85\%$
10	Afara et al., 2014 (97)	6,113–5,446	OA models in rats ($N = 36$)	Mankin score component: Structural integrity	$R^2 = 94.78\%$
11	Afara et al., 2014 (97)	10,500–7500	OA models in rats ($N = 36$)	Mankin score component: Cellularity	$R^2 = 88.03\%$
12	Afara et al., 2014 (97)	12,436–9,967	OA models in rats ($N = 36$)	Mankin score component: Safain-O-staining	$R^2 = 96.39\%$
13	Sarin et al., 2016 (102)	9,524–14,286	Equine joints ($N = 44$)	Thickness	$R^2 = 70.3\%$
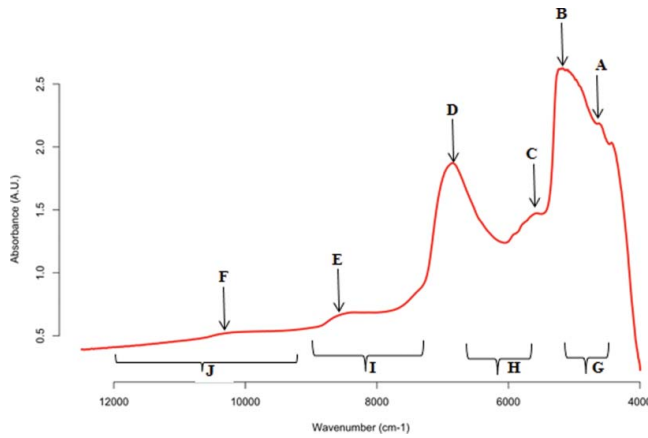
Figure 1. Typical NIR spectra of rat articular cartilage indicating specific absorption peaks (A–F) and spectral regions (G–J) associated with the matrix components and properties of articular cartilage.

Characterization of articular cartilage integrity: Quantifying injury and degeneration

In addition to analysis for determination of the micro- and macroscopic properties of articular cartilage using NIR spectroscopy, the method has also been proposed and applied for the quantification of cartilage injury, and a potential means of scoring cartilage injuries in real-time during joint surgery. Currently, cartilage injuries (lesions) are scored arthroscopically according to the International Cartilage Repair Society (ICRS) scoring system (109), which is based on the relative depth of the injury. However, this method has been shown to be poorly reproducible and repeatable (32, 110, 111) due to user subjectivity. Thus, NIR spectroscopy has been proposed as a potential method for objective scoring of cartilage defect. In this review, we highlight quantitative scoring parameters that have been defined based on cartilage NIR spectrum.

Primary assessment

Function score

This function employs differences in absorbance peaks to generate a score with the aim of differentiating between normal and degenerated cartilage. The function score is of the form $\chi = \sum_{n}^{i=1} C_i A_{\lambda i}$, where χ is a scaled outcome between 0 and 1, with 1 representing normal tissue and 0 degenerated tissue. C_i is the coefficient assigned to the wavenumber of interest and $A_{\lambda i}$ is the absorbance measured at each wavenumber of interest. The score has proven to have successfully quantify degeneration in articular cartilage (89, 112).

Water–amide ratio

This parameter, introduced by Spahn et al. (40), is the ratio (AR) of the magnitude of the absorbance peaks of amide-water band (first OH and CH combination overtones) to the amide band (second CH overtones), and quantifies the water content in cartilage (40, 72, 89). The parameter is based on the understanding that degeneration results in increase water content in cartilage. The ratio is calculated as

Table 5. NIR spectral peaks (A–F) and regions (G–J) identified with the matrix components of articular cartilage, together with the associated peak assignments. Spectral regions without text identification consist of a combination of multiple spectral regions in Figure 1.

S/N	Author(s)	Spectral region, wavenumber (cm^{-1})	Assignment	Tissue component
1	Afara et al., 2013 (79)	5,623 (**C**)	Not specified	PGs + water
2	Afara et al., 2013 (79), Afara et al., 2012 (74)	6,667–7,142	Water saturation	Excluded from analysis
3	Afara et al., 2013 (79)	7,500–12,500	Polymer-type chain network	PGs + collagen
4	Afara et al., 2013 (39)	7,200–8,850 (**I**)	2nd CH overtones	Collagen
5	Afara et al., 2013 (39)	5,300–8,850	1st and 2nd CH and OH overtones	PGs + collagen + water
6	Afara et al., 2013 (79)	5,700–6,100	1st CH and SH overtones	PGs
8	McGoverin et al., 2016 (100)	4,310	Not specified	PGs
9	McGoverin et al., 2016 (100), Padalkar et al., 2013 (93), McGoverin et al., 2014 (95)	5,200 (**B**)	Not specified	Bound + free water
10	Padalkar et al., 2013 (93)	6,890 (**D**)	Not specified	Free water
11	Palukuru et al., 2014 (96)	4,020	C—H stretch and C—C stretch combination	PGs
12	Padalkar et al., 2013 (93), Palukuru et al., 2014 (96)	4,310	Combination of C—H stretch and CH_2 deformation vibration	PGs
13	Palukuru et al., 2014 (96)	4,260	CH_2 bending vibration and 2nd overtone	Collagen
14	Palukuru et al., 2014 (96)	4,610 (**A**)	Asymmetric C—H stretch and C—H deformation	Collagen
15	Palukuru et al., 2014 (96)	4,890	N–H in plane bending vibration	Collagen
16	Afara et al., 2012 (74), Afara et al., 2014 (97)	5,446–6,102	1st overtone CH_n and SH absorption	PGs + collagen
17	Afara et al., 2012 (74), Afara et al., 2014 (97)	5,150		Water
18	Afara et al., 2012 (74), Afara et al., 2014 (97)	4,600–4,900 (**G**)	Amide combinations and overtones	PGs + collagen
19	McGoverin et al., 2014 (95)	8,645 (**E**)	Not specified	Collagen
20	McGoverin et al., 2014 (95)	7,000	Not specified	Free water
21	Afara et al., 2014 (98)	9,959–12,489	3rd overtone CH_n and ROH vibrations	PGs
22	Afara et al., 2014 (98)	5,440–6,450 (**H**)	1st overtone CH_n and SH vibrations	PGs
24	Afara et al., 2014 (97)	9,967–12,436	3rd overtone vibration	Collagen
25	Afara et al., 2015 (44)	9,091–12,500 (**J**)	3rd overtone OH vibration	PGs + collagen
26	Afara et al., 2015 (44)	10,309 (**F**)	Not specified	Water

AR = NIR absorption at 7,017 cm^{-1}/NIR absorption at 8,510 cm^{-1}. (40)

AR is lowest in normal cartilage (Grade 0), and highest in fully degenerated cartilage (Grade 3). This parameter was utilized by Spahn et al. (40, 72) to discriminate among normal, grade 1, and grade 2 cartilage defects in human joints.

Shift in frequency of water absorbance peaks

Two dominant water peaks are observable in the NIR spectral region, one centered at 5,200 cm^{-1}, attributed to free and bound water (113) and the other at 6,890 cm^{-1}, attributed to free water (114). It is known that water in cartilage can be free, tightly bound to collagen, or loosely bound to PGs (93). More so, since cartilage integrity is strongly correlated to changes in total water content of its matrix, knowledge of the relative water content, both free and bound water, could be used as an indicator of cartilage tissue integrity. During cartilage degeneration, the water peak centered at 5,200 cm^{-1} has been observed to undergo a

slight shift to higher frequency (lower wavenumber). As the frequency of vibration depends on the mobility of water, a shift to higher frequency means more mobile free water and less mobile bound water (93). This spectral behavior due to articular cartilage water content, detailed by Padalkar et al. (93), can be utilized as a parameter to evaluate early-stage cartilage degeneration, which often occurs without any observable/visible changes in the tissue.

Secondary assessment: Spectral pre-processing and multivariate analyses

The non-specificity of NIR spectral peaks, owing to overlapping peaks, poses a major limitation for the application of this optical technique. In addition, NIR spectral response of biological materials with high water content (like articular cartilage) tends to suffer from the overwhelming effect of water, which significantly absorbs NIR light (115) leading to spectral saturation and masking of peaks related to cartilage matrix components, thereby impeding spectral interpretation. Nevertheless, these limitations are easily addressed by selecting appropriate optical window during analysis (highlighted in Tables 1–5), together with application of spectral pre-processing (116–118) and multivariate analytical method, such as principal component analysis (PCA) (119, 120) and partial least square (PLS) regression (121, 122), in order to extract relevant subtle information from the spectral data.

The application of multivariate statistical/analytical methods for analysis of NIR spectra (chemometrics) has become a standard in fields of study and industry where NIR spectroscopy is employed for analyses and quality control of products, such as in pharmaceuticals (123). The goal of such multivariate spectral analyses is often to classify the samples based on similar spectral features, or to predict certain physical or chemical properties of samples from their spectra. The classification techniques that have been utilized for analyses of NIR spectra include feature extraction and dimension reduction techniques like PCA (120), and other algorithms like discriminant analysis (DA) (124), soft independent modeling of class analogy (SIMCA) (125), support vector machines (SVM), etc. For prediction, multivariate regression techniques are employed to develop predictive models which establish a linear relationship between the spectral data (independent variables or predictors) and reference values (dependent variables or response). Methods such as multiple linear regression (MLR), principal component regression (PCR), and PLS regression are common for analysis of NIR spectra.

Since the accuracy and performance of classification or prediction based on NIR spectra is significantly influenced by the choice of spectral pre-processing performed prior to analyses, it is critical to select the right pre-processing algorithm that would optimize classification/ prediction. Spectral pre-processing techniques are generally employed for scatter correction and/or spectral transformation, such as derivative pre-treatment. Common spectral pre-processing algorithms include normalization, standard normal variate (SNV), multiplicative scatter correction (MSC), and derivatives, particularly first and second derivatives. Derivative pre-processing is effective for eliminating spectral baseline, since the derivative of any function eliminates constant variables, as well as amplifying subtle changes in the spectra, such as extracting information from partially masked peaks (shoulders). In Table 6, we highlight the common spectral preprocessing, classification, and prediction methods that have been employed in the analyses of NIR spectra of articular cartilage, with the corresponding cartilage property under study.

Table 6. Review of spectral pre-processing and multivariate analysis of NIR spectra of articular cartilage.

S/N	Authors	Cartilage property	Pre-processing	Classification	Regression
1	Afara et al., 2012a (74)	Mankin score	1D, SNV	PCA	PLS
3	Afara et al., 2014a (98)	PG content	SLS	PCA	PLS
4	Afara et al., 2014b (97)	Structural integrity, cellularity, and matrix staining	SLS	PCA, DA	PLS
5	Afara et al., 2013 (39)	Thickness	MSC, SNV, WD	PCA	PLS
6	Afara et al., 2013 (79)	reswelling	SNV	PCA	PLS
7	Afara et al., 2015 (44)	Biochemical, biomechanical, and histological	2D	none	PLS
8	Afara et al., 2016 (103)	Elastic rebound	MSC, 1D	none	PLS
9	Padalkar et al., 2013 (93)	Water content	MSC, 2D	none	PLS
10	Mc Goverin et al., 2014 (95)	Thickness and modified Mankin grade	SNV, 2D	PCA	PLS
11	Mc Goverin et al., 2016 (100)	Water, PG, and collagen content	Extended MSC, normalization, 2D	none	PLS
12	Brown et al. 2009 (87)	PG depletion	1D, 2D	PCA	PLS
13	Palukuru et al., 2014 (96)	Collagen and chondroitn sulphate content	Extended MSC, 2D	none	PLS
14	Palukuru et al., 2016 (101)	PG and collagen content	2D	none	PLS
15	Baykal et al., 2010 (85)	PG and collagen content	MSC, 1D	none	PLS
16	Sarin et al., 2016 (102)	Cartilage thickness, equilibrium modulus, and instantaneous modulus	2D	none	PLS

Notes: SNV = standard normal variate; PCA = principal component analysis; PLS = partial least squares; 1D = 1st derivative; 2D = 2nd derivative; SLS = straight line subtraction; DA = discriminant analysis; WD = wavelet detrending; MSC = multiplicative scatter correction.

Clinical application of NIR spectroscopy for cartilage evaluation

So far, only a few researches have been published on the clinical applications of NIR spectroscopy for articular cartilage assessment. Nevertheless, it is worth noting that application of this optical technique for evaluation of cartilage integrity is fairly recent, less than a decade. The flexibility of NIR spectroscopy enables easy adaptability of the technique for arthroscopic evaluation of cartilage. More so, development of NIR fibre optic probes with similar design as traditional arthroscopic hooks, allows for easy application of this technique during arthroscopic surgery. This is the approach of the arthrospec-one NIR arthroscopic probe (Arthrospec GmbH, Jena, Germany), first applied by Spahn and coworkers (40, 83, 84, 86, 92).

Table 7 highlights the literature on clinical application of NIR for characterization of articular cartilage injury, defects, and integrity in human joints.

The outcome of their studies suggests that NIR is an effective tool for cartilage lesions differentiation (92), detection, and analysis of initial cartilage pathology (84), evaluation of low grade lesion (40), and determination of cartilage mechanical properties (86) in real-time during arthroscopic surgery.

The probe has 1 mm diameter tip, with six peripherally arranged optical fibres for illumination, and one centrally positioned fibre for detection. A major challenge in the clinical application of NIR spectroscopy involves handling of the probe during spectral measurement, as factors such as probe vibration, sufficient contact, and correct vertical positioning with respect to the tissue surface in the region of interest can affect the accuracy of acquired spectral data (39, 79). Nevertheless, with the availability of optical systems with fast and near-instant optical detectors capable of spectral measurements within micro-seconds,

Table 7. A systematic and chronological literature review of the application of NIR spectroscopy for evaluation of articular cartilage.

S/N	Author(s)	Specimen and methodology	Spectral region, wavenumber (cm^{-1})	Results
1	Spahn et al., 2007 (40)	Patients ($N = 12$) suffering from knee pain for over 3 months.	5,882–9,091	NIRS has a significantly ($p = 0.000$) higher specificity (0.96) and accuracy (0.98) than MRI (0.54 and 0.70, respectively).
2	Spahn et al., 2010 (83)	Patients ($N = 15$) undergoing arthroscopic knee operations.	5,882–11,111	NIRS shows a significant ($p < .001$) correlation within the observers of $R = 0.885 \pm 0.036$.
3	Hofmann et al., 2010 (84)	Patients ($N = 21$) with knee pain lasting for half a year.	6,780–8,696	Significant ($p > .007$) correlations with three KOOS sub-scores only were found with NIRS. The Spearman's rank correlation coefficient ranged between 0.68 and 0.72.
4	Marticke et al., 2010 (86)	Patients ($N = 32$) undergoing arthroscopic knee operations.	5,882–9,091	Significant correlation between NIRS-absorption and ICRS grade ($R = 0.467$) and Young's Modulus ($R = 0.535$).
5	Spahn et al., 2013 (92)	Patients with degenerative knee ($N = 6$) versus traumatic knee ($N = 6$).	5,882–11,111	The mean NIR absorption value of 71.5 was obtained for traumatic knee, and 31.7 for degenerative knee.

Study type: E = experimental; C = clinical, N = number of patients.
Only studies that have used spectral data within the IUPAC defined wavenumber region are considered: 4,000–12,500 cm^{-1} = 2,500–800 nm.

and sufficient training, these limitations can be minimized. In addition to the ease of coupling NIR spectroscopy with traditional arthroscopy, the rapid action of this optical technique enables real-time evaluation and decision-making during joint surgery.

The occurrence of varying degrees of lesions is evident in 63% of knees undergoing arthroscopy surgery (126–128). Thus, accurate quantitative evaluation and qualitative grading of cartilage lesions is crucial for decision-making during and after surgery. When fully developed and optimized, NIR arthroscopy is likely to significantly improve the accuracy of arthroscopic outcome, and revolutionize the way traditional arthroscopy is performed clinically.

Open questions and future directions

Considering existing research on the application of NIR spectroscopy for evaluation of articular cartilage, there are still a number of open questions and future work that need to be addressed and undertaken before this optical technique can become a standard method for both clinical and laboratory assessment of articular cartilage. These questions and future work are outlined below:

1. There is still need for an in-depth understanding of the interaction between the NIR light and cartilage properties, in order to understand the specific contribution of the different components of the tissue to the overall spectra. This would allow for accurate quantification of cartilage components and determination of tissue degeneration. This can potentially be addressed using simulation approach.
2. What is the contribution of the different cartilage layers to its overall spectrum? This is important as the collagen orientation, PG, and water content are depth-dependent

(i.e., layer-dependent) and influence the functional response and health of the tissue. For example, understanding the effect of the collagen network birefringence on the spectral response may provide insight that may be essential for early-stage detection of cartilage degeneration.

3. What is the contribution of the subchondral bone to the overall spectral output of osteochondral samples? This understanding may enable characterization of subchondral bone pathologies using NIR spectroscopy.

4. Can NIR spectroscopy be combined with other fast and non-destructive techniques such as OCT and high frequency ultrasound for evaluation of articular cartilage and subchondral bone? This multimodality approach could enable quantitative characterization and imaging of cartilage and subchondral bone during surgery.

Funding

References

1. Mow, V. C., and Huiskes, R. (2005) *Basic orthopaedic biomechanics & mechano-biology.* Lippincott Williams & Wilkins, Philadelphia.
2. Hunziker, E. B. (2002) Articular cartilage repair: Basic science and clinical progress. A review of the current status and prospects. *Osteoarth. Cart.* 10(6): 432–463.
3. Mow, V. C., and Guo, X. E. (2002) Mechano-electrochemical properties of articular cartilage: Their inhomogeneities and anisotropies. *Annu. Rev. Biomed. Eng.* 4: 175–209.
4. Mayne, R. (1989) Cartilage collagens. What is their function, and are they involved in articular disease? *Arthritis. Rheum.* 32(3): 241–246.
5. Hardingham, T. E., and Fosang, A. J. (1992) Proteoglycans: Many forms and many functions. *FASEB J.* 6(3): 861–870.
6. Jaffe, F. F., Manki, N. H. J., Weiss, C., and Zarins, A. (1974) Water binding in the articular cartilage of rabbits. *J. Bone Joint Surg. Am.* 56(5): 1031–1039.
7. Muir, H. (1995) The chondrocyte, architect of cartilage. Biomechanics, structure, function and molecular biology of cartilage matrix macromolecules. *BioEssays.* 17(12): 1039–1048.
8. Kellgren, J., and Lawrence, J. (1957) Radiological assessment of osteoarthritis. *Ann. Rheum. Dis.* 16: 494.
9. Mankin, H. J., Dorfman, H., Lippiello, L., and Zarins, A. (1971) Biochemical and metabolic abnormalities in articular cartilage from osteo-arthritic human hips. II. Correlation of morphology with biochemical and metabolic data. *J. Bone Joint Surg. Am.* 53(3): 523–537.
10. Sandell, L. J., and Aigner, T. (2001) Articular cartilage and changes in arthritis: Cell biology of osteoarthritis. *Arthritis Res. BioMed Central* 3(2): 107.
11. Buckwalter, J. A., and Mankin, H.J. (1997) Instructional course lectures, the American academy of orthopaedic surgeons—Articular cartilage. Part II: Degeneration and osteoarthrosis, repair, regeneration, and transplantation. *J. Bone & Jt. Surg.* 79(4): 612–632.
12. Saarakkala, S., Julkunen, P., Kiviranta, P., Mäkitalo, J., Jurvelin, J. S., and Korhonen, R. K. (2010) Depth-wise progression of osteoarthritis in human articular cartilage: Investigation of composition, structure and biomechanics. *Osteoarth. Cart.* 18(1): 73–81.
13. Guilak, F., Ratcliffe, A., Lane, N., Rosenwasser, M. P., and Mow, V. C. (1994) Mechanical and biochemical changes in the superficial zone of articular cartilage in canine experimental osteoarthritis. *J Orthop Res.* 12(4): 474–484.
14. Armstrong, C. G., and Mow, V. C. (1982) Variations in the intrinsic mechanical properties of human articular cartilage with age, degeneration, and water content. *J Bone Joint Surg Am.* 64(1): 88–94.

15. Mankin, H. J., and Thrasher, A. Z. (1975) Water content and binding in normal and osteoar-thritic human cartilage. *J Bone Joint Surg Am.* 57(1): 76–80.

16. Torzilli, P. A., Rose, D. E., and Dethmers, D. A. (1982) Equilibrium water partition in articular cartilage. *Biorheology* 19(4): 519–537.

17. Croft, P. (2005) An introduction to the Atlas of Standard Radiographs of Arthritis. *Rheumatology* 44(4): 27–32.

18. Scott, D., and Gishen, P. (1999) Radiological assessment of hip osteoarthritis. *Lancet* 353(9147): 87–88.

19. Altman, R. D., Fries, J. F., Bloch, D. A., Carstens, J., Cooke, T. D, Genant, H., Fries, J. F., Gofton, P., Groth, H., McShane, D. J., Murphy, W. A., et al. (1987) Radiographic assessment of progression in osteoarthritis. *Arthritis Rheum.* 30: 1214–1225.

20. Gupta, K. B., Duryea, J., and Weissman, B. N. (2004) Radiographic evaluation of osteoarthritis. *Radiologic Clin. N. Am.* 42: 11–41.

21. Borthakur, A., Shapiro, E. M., Beers, J., Kudchodkar, S., Kneeland, J. B., and Reddy, R. (2000) Sensitivity of MRI to proteoglycan depletion in cartilage: Comparison of sodium and proton MRI. *Osteoarthr Cartil.* 8(4): 288–293.

22. Tiderius, C. J., Olsson, L. E., Leander, P., Ekberg, O., and Dahlberg, L. (2003) Delayed gadolinium-enhanced MRI of cartilage (dGEMRIC) in early knee osteoarthritis. *Magn Reson Med.* 49 (3): 488–492.

23. van Tiel, J., Bron, E. E., Bos, P. K., Klein, S., Reijman, M., Verhaar, J. A., Tiderius, C. J., Krestin, G. P., Weinans, H., Kotek, G., and Oei, E. H. G. (2012) Reproducibility of 3D delayed gadolinium enhanced MRI of cartilage (DGEMRIC) of the knee at 3.0 Tesla in patients with early-stage osteoarthritis. *Osteoarthr Cartil.* 20: S230–S231.

24. Kurkijärvi, J. E., Nissi, M. J., Kiviranta, I., Jurvelin, J. S., and Nieminen, M. T. (2004) Delayed gadolinium-enhanced MRI of cartilage (dGEMRIC) and T2 characteristics of human knee articular cartilage: Topographical variation and relationships to mechanical properties. *Magn Reson Med.* 52(1): 41–46.

25. Williams, A., Sharma, L., McKenzie, C. A., Prasad, P. V., and Burstein, D. (2005) Delayed gadolinium-enhanced magnetic resonance imaging of cartilage in knee osteoarthritis: Findings at different radiographic stages of disease and relationship to malalignment. *Arthritis Rheum.* 52(11): 3528–3535.

26. Choi, J.-A., and Gold, G. E. (2011) MR imaging of articular cartilage physiology. *Magn Reson Imaging Clin N Am.* 19(2): 249–282.

27. Sanders, T. G. (2011) Imaging of the postoperative knee. *Semin Musculoskelet Radiol.* 15(4): 383–407.

28. Gope, Z. A. G., and Kavanagh, E. C. (2006) MR imaging of the postoperative meniscus: Repair, resection, and replacement. *Semin Musculoskelet Radiol.* 10(3): 229–240.

29. Bae, D. K., Yoon, K. H., and Song, S. J. (2006) Cartilage healing after microfracture in osteoarthritic knees. *Arthrosc - J Arthrosc Relat Surg.* 22(4): 367–374.

30. Gooding, C. R., Bartlett, W., Bentley, G., Skinner, J. A., Carrington, R., and Flanagan, A. (2006) A prospective, randomised study comparing two techniques of autologous chondrocyte implantation for osteochondral defects in the knee: Periosteum covered versus type I/III collagen covered. *Knee* 13(3): 203–210.

31. Briggs, T. W. R., Mahroof, S., David, L. A., Flannelly, J., Pringle, J., and Bayliss, M. (2003) Histological evaluation of chondral defects after autologous chondrocyte implantation of the knee. *J Bone Jt Surg [Br].* 85(7): 1077–1083.

32. Brismar, B. H., Wredmark, T., Movin, T., Leandersson, J., and Svensson, O. (2002) Observer reliability in the arthroscopic classification of osteoarthritis of the knee. *J Bone Joint Surg Br.* 84(1): 42–47.

33. Wright, R. W. (2014) Osteoarthritis classification scales: Interobserver reliability and arthroscopic correlation. *J Bone Joint Surg Am.* 96(14): 1145–1151.

34. Ayral, X., Gueguen, A., Ike, R. W., Bonvarlet, J. P., Frizziero, L., Kalunian, K., Moreland, L. W., Myers, S., O'Rourke, K. S., Roos, H., Altman, R., and Dougados, M. (1998) Inter-observer reliability of the arthroscopic quantification of chondropathy of the knee. *Osteoarth. Cart.* 6(3): 160–166.

35. Hunt, N., Sanchez-Ballester, J., Pandit, R., Thomas, R., and Strachan, R. (2001) Chondral lesions of the knee: A new localization method and correlation with associated pathology. *Arthroscopy* 17(5): 481–490.

36. Hui, A. C. W., Javed, A., Siddique, M., and Vaghela, M. (2002) Interobserver variations in intra-articular evaluation during arthroscopy of the knee. *Sr House Off J Bone Jt Surg [Br]*. 84: 48–49.

37. Jerosch, J., Castro, W. H., de Waal Malefijt, M. C., Busch, M., and van Kampen, A. (1997) [Inter-observer variation in diagnostic arthroscopy of the knee joint. "How really objective are arthro-scopic findings?"]. *Unfallchirurg* 100(10): 782–786.

38. Oakley, S. P., Portek, I., Szomor, Z., Turnbull, A., Murrell, G. A. C., Kirkham, B. W., and Lassere, M. N. (2002) Poor accuracy and interobserver reliability of knee arthroscopy measurements are improved by the use of variable angle elongated probes. *Ann Rheum Dis.* 61(6): 540–543.

39. Afara, I., Singh, S., and Oloyede, A. (2013) Application of near infrared (NIR) spectroscopy for determining the thickness of articular cartilage. *Med Eng Phys.* 35(1): 88–95.

40. Spahn, G., Plettenberg, H., Kahl, E., Klinger, H. M., Mückley, T., and Hofmann, G. O. (2007) Near-infrared (NIR) spectroscopy. A new method for arthroscopic evaluation of low grade degenerated cartilage lesions. Results of a pilot study. *BMC Musculoskelet Disord.* 8: 47.

41. Esmonde-White, K. A., Esmonde-White, F. W. L., Morris, M. D., and Roessler, B. J. (2011) Fiber-optic Raman spectroscopy of joint tissues. *Analyst* 136(8): 1675–1685.

42. Takahashi, Y., Sugano, N., Takao, M., Sakai, T., Nishii, T., and Pezzotti, G. (2014) Raman spectroscopy investigation of load-assisted microstructural alterations in human knee cartilage: Preliminary study into diagnostic potential for osteoarthritis. *J Mech Behav Biomed Mater.* 31: 77–85.

43. te Moller, N. C. R., Brommer, H., Liukkonen, J., Virén, T., Timonen, M., Puhakka, P. H., Jurvelin, J. S., van Weeren, P. R., and Töyräs, J. (2013) Arthroscopic optical coherence tomography provides detailed information on articular cartilage lesions in horses. *Vet J.* 197(3): 589–595.

44. Afara, I. O., Hauta-Kasari, M., Jurvelin, J. S., Oloyede, A., and Töyräs, J. (2015) Optical absorption spectra of human articular cartilage correlate with biomechanical properties, histological score and biochemical composition. *Physiol Meas.* 36(9): 1913–1928.

45. Chu, C. R., Williams, A., Tolliver, D., Kwoh, C. K., Bruno, S., and Irrgang, J. J. (2010) Clinical optical coherence tomography of early articular cartilage degeneration in patients with degenerative meniscal tears. *Arthritis Rheum.* 62(5): 1412–1420.

46. Ugryumova, N., Stevens-Smith, J., Scutt, A., and Matcher, S. J. (2008) Local variations in bone mineral density: A comparison of OCT versus x-ray micro-CT. In *Coherence domain optical methods and optical coherence tomography in Biomedicine XII*, Proceedings of SPIE (6847), Izatt, J. A., Fujimoto, J. G., Tuchin, V. V., Eds., SPIE, San Jose, CA, pp. 684–725.

47. Potter, K., Kidder, L. H., Levin, I. W., Lewis, E. N., and Spencer, R. G. (2001) Imaging of collagen and proteoglycan in cartilage sections using Fourier transform infrared spectral imaging. *Arthritis Rheum.* 44(4): 846–855.

48. Camacho, N. P., West, P., Torzilli, P. A., and Mendelsohn, R. (2001) FTIR microscopic imaging of collagen and proteoglycan in bovine cartilage. *Biopolymers.* 62(1): 1–8.

49. David-Vaudey, E., Burghardt, A., Keshari, K., Brouchet, A., Ries, M., and Majumdar, S. (2005) Fourier transform infrared imaging of focal lesions in human osteoarthritic cartilage. *Eur Cell Mater.* 10: 51–60; discussion 60.

50. Xia, Y., Ramakrishnan, N., and Bidthanapally, A. (2007) The depth-dependent anisotropy of articular cartilage by Fourier-transform infrared imaging (FTIRI). *Osteoarth. Cart.* 15(7): 780–788.

51. Li, G., Thomson, M., Dicarlo, E., Yang, X., Nestor, B., Bostrom, M. P. G., and Camacho, N. P. (2005) A chemometric analysis for evaluation of early-stage cartilage degradation by infrared fiber-optic probe spectroscopy. *Appl Spectrosc.* 59(12): 1527–1533.

52. West, P. A., Bostrom, M. P. G., Torzilli, P. A., and Camacho, N. P. (2004) Fourier transform infrared spectral analysis of degenerative cartilage: an infrared fiber optic probe and imaging study. *Appl Spectrosc.* 58(4): 376–381.

53. Kim, M., Bi, X., Horton, W. E., Spencer, R. G., and Camacho, N. P. (2016) Fourier transform infrared imaging spectroscopic analysis of tissue engineered cartilage: histologic and biochemical correlations. *J Biomed Opt.* 10(3): 031105.

54. Töyräs, J., Nieminen, H. J., Laasanen, M. S., Nieminen, M. T., Korhonen, R. K., Rieppo, J., Hirvonen, J., Helminen, H. J., and Jurvelin, J. S. (2002) Ultrasonic characterization of articular cartilage. *Biorheology* 39(1–2): 161–169.

55. Nieminen, H. J., Zheng, Y., Saarakkala, S., Wang, Q., Toyras, J., Huang, Y., and Jurvelin, J. (2009) Quantitative assessment of articular cartilage using high-frequency ultrasound: Research findings and diagnostic prospects. *Crit Rev Biomed Eng.* 37(6): 461–494.

56. Kaleva, E., Virén, T., Saarakkala, S., Sahlman, J., Sirola, J., Puhakka, J., Paatela, T., Kröger, H., Kiviranta, I., Jurvelin, J. S., and Töyräs, J. (2011) Arthroscopic ultrasound assessment of articular cartilage in the human knee joint: A potential diagnostic method. *Cartilage* 2(3): 246–253.

57. Herschel, W. (1800) Experiments on the refrangibility of the invisible rays of the sun. *Philos Trans R Soc London.* 90: 284–292.

58. Miller, C. E. (2001) Chemical principles of near-infrared technology. In *Near-infrared technology in agricultural and food industries*, Williams, P., and Norris, K. H., Eds., AACC International, St. Paul, MN, pp. 19–37.

59. Rendell, M., Anderson, E., Schlueter, W., Mailliard, J., Honigs, D., and Rosenthal, R. (2003) Determination of hemoglobin levels in the finger using near infrared spectroscopy. *Clin Lab Haematol.* 25(2): 93–97.

60. Ferrari, M., Wilson, D. A., Hanley, D. F., Hartmann, J. F., and Traystman, R. J. (1989) Determination of cerebral venous hemoglobin saturation by derivative near infrared spectrosocpy. *Adv Exp Med Biol.* 248: 47–53.

61. Moreno, P. R., Lodder, R. A., Purushothaman, K. R., Charash, W. E., O'Connor, W. N., and Muller, J. E. (2002) Detection of lipid pool, thin fibrous cap, and inflammatory cells in human aortic atherosclerotic plaques by near-infrared spectroscopy. *Circulation* 105(8): 923–927.

62. Lin, T. P., and Hsu, C. C. Determination of residual moisture in lyophilized protein pharmaceuticals using a rapid and non-invasive method: Near infrared spectroscopy. *PDA J Pharm Sci Technol.* 56(4): 196–205.

63. Šašić, S., and Ozaki, Y. (2001) Short-wave near-infrared spectroscopy of biological fluids. 1. Quantitative analysis of fat, protein, and lactose in raw milk by partial least-squares regression and band assignment. *Anal Chem.* 73(1): 64–71.

64. Shaw, R. A., Kotowich, S., Mantsch, H. H., and Leroux, M. (1996) Quantitation of protein, creatinine, and urea in urine by near-infrared spectroscopy. *Clin Biochem.* 29(1): 11–19.

65. Gu, Y., Chen, W. R., Xia, M., Jeong, S. W., and Liu, H. (2016) Effect of photothermal therapy on breast tumor vascular contents: Noninvasive monitoring by near-infrared spectroscopy. *Photochem Photobiol.* 81(4): 1002–1009.

66. Ali, J. H., Wang, W. B., Zevallos, M., and Alfano, R. R. (2004) Near infrared spectroscopy and imaging to probe differences in water content in normal and cancer human prostate tissues. *Technol Cancer Res Treat.* 3(5): 491–497.

67. Sämann, A., Fischbacher, C. H., Jageman, N. K. U., Danzer, K., Schüler, J., Papenkordt, L., and Müller, U. A. (2000) Non-invasive blood glucose monitoring by means of near infrared spectroscopy: Investigation of long-term accuracy and stability. *Exp Clin Endocrinol Diabetes* 108(6): 406–413.

68. Petibois, C., Melin, A.-M., Perromat, A., Cazorla, G., and Déléris, G. (2000) Glucose and lactate concentration determination on single microsamples by Fourier-transform infrared spectroscopy. *J Lab Clin Med.* 135(2): 210–215.

69. Zeller, H., Novak, P., and Landgraf, R. (1989) Blood glucose measurement by infrared spectroscopy. *Int J Artif Organs.* 12(2): 129–135.

70. Shaw, R. A., Kotowich, S., Eysel, H. H., Jackson, M., Thomson, G. T., and Mantsch, H. H. (1995) Arthritis diagnosis based upon the near-infrared spectrum of synovial fluid. *Rheumatol Int.* 15 (4): 159–165.

71. Caplan, J. D., Waxman, S., Nesto, R. W., and Muller, J. E. (2006) Near-infrared spectroscopy for the detection of vulnerable coronary artery plaques. *J Am Coll Cardiol.* 47(8 Suppl.): C92–C96.

72. Spahn, G., Plettenberg, H., Nagel, H., Kahl, E., Klinger, H. M., Mückley, T., Günther, M., Hofmann, G. O., and Mollenhauer, J. A. (2008) Evaluation of cartilage defects with near-infrared spectroscopy (NIR): An ex vivo study. *Med Eng Phys.* 30(3): 285–292.

73. Lu, L., Cai, J., and Fros, T. R. L. (2010) Near infrared spectroscopy of stearic acid adsorbed on montmorillonite. *Spectrochim Acta A Mol Biomol Spectrosc.* 75(3): 960–963.

74. Afara, I., Prasadam, I., Crawford, R., Xiao, Y., and Oloyede, A. (2012) Non-destructive evaluation of articular cartilage defects using near-infrared (NIR) spectroscopy in osteoarthritic rat models and its direct relation to Mankin score. *Osteoarth. Cart.* 20(11): 1367–1373.

75. Afara, I. O., Pawlak, Z., and Oloyede, A. (2011) Current state of the application of infrared optical methods for assessing articular cartilage. *J Mater Sci Eng A.* 1(6): 1–7.

76. Blanco, M., and Villarroya, I. (2002) NIR spectroscopy: A rapid-response analytical tool. *TrAC Trends Anal Chem.* 21(4): 240–250.

77. Villringer, A., Planck, J., Hock, C., Schleinkofer, L., and Dirnagl, U. (1993) Near infrared spectroscopy (NIRS): A new tool to study hemodynamic changes during activation of brain function in human adults. *Neurosci Lett.* 154(1–2): 101–104.

78. Lammertyn, J., Peirs, A., De Baerdemaeker, J., and Nicolaï, B. (2000) Light penetration properties of NIR radiation in fruit with respect to non-destructive quality assessment. *Postharvest Biol Technol.* 18(2): 121–132.

79. Afara, I. O., Singh, S., and Oloyede, A. (2013) Load-unloading response of intact and artificially degraded articular cartilage correlated with near infrared (NIR) absorption spectra. *J Mech Behav Biomed Mater.* 20: 249–258.

80. Faris, F., Thorniley, M., Wickramasinghe, Y., Houston, R., Rolfe, P., Livera, N., and Spencer, A. (1991) Non-invasive in vivo near-infrared optical measurement of the penetration depth in the neonatal head. *Clin Phys Physiol Meas.* 12(4): 353–358.

81. Afara, I. O., Prasadam, I., Crawfor, D. R., Xiao, Y., and Oloyede, A. (2013) Near infrared (NIR) absorption spectra correlates with subchondral bone micro-CT parameters in osteoarthritic rat models. *Bone* 53(2): 350–357.

82. Brown, C. P., Bowden, J. C., Rintoul, L., Meder, R., Oloyede, A., and Crawford, R. W. (2009) Diffuse reflectance near infrared spectroscopy can distinguish normal from enzymatically digested cartilage. *Phys Med Biol.* 54(18): 5579–5594.

83. Spahn, G., Klinger, H. M., Baums, M., Hoffmann, M., Plettenberg, H., Kroker, A., and Hofmann, G. O. (2010) Near-infrared spectroscopy for arthroscopic evaluation of cartilage lesions: Results of a blinded, prospective, interobserver study. *Am J Sports Med.* 38(12): 2516–2521.

84. Hofmann, G. O., Marticke, J., Grossstück, R., Hoffmann, M., Lange, M., Plettenberg, H. K. W., Braunschweig, R., Schilling, O., Kaden, I., and Spahn, G. (2010) Detection and evaluation of initial cartilage pathology in man: A comparison between MRT, arthroscopy and near-infrared spectroscopy (NIR) in their relation to initial knee pain. *Pathophysiology* 17(1): 1–8.

85. Baykal, D., Irrechukwu, O., Lin, P. C., Fritton, K., Spencer, R. G., and Pleshko, N. (2010) Nondestructive assessment of engineered cartilage constructs using near-infrared spectroscopy. *Appl Spectrosc.* 64(10): 1160–1166.

86. Marticke, J. K., Hösselbarth, A., Hoffmeier, K. L., Marintschev, I., Otto, S., Lange, M., Plettenberg, H. K., Spahn, G., and Hofmann, G. O. (2010) How do visual, spectroscopic and biomechanical changes of cartilage correlate in osteoarthritic knee joints? *Clin Biomech (Bristol, Avon).* 25(4): 332–340.

87. Brown, C. P., Bowden, J. C., Rintoul, L., Meder, R., Oloyede, A., and Crawford, R. W. (2009) Diffuse reflectance near infrared spectroscopy can distinguish normal from enzymatically digested cartilage. *Phys Med Biol.* 54(18): 5579–5594.

88. Johansson, A., Sundqvist, T., Kuiper, J.-H., and Öberg, P. Å. (2011) A spectroscopic approach to imaging and quantification of cartilage lesions in human knee joints. *Phys Med Biol.* 56(6): 1865–1878.

89. Brown, C. P., Oloyede, A., Crawford, R. W., Thomas, G. E. R., Price, A. J., and Gill, H. S. (2012) Acoustic, mechanical and near-infrared profiling of osteoarthritic progression in bovine joints. *Phys Med Biol.* 57(2): 547–559.

90. Hoffmann, M., Lange, M., Meuche, F., Reuter, T., Plettenberg, H., Spahn, G., and Ponomare, V. I.. (2012) Comparison of optical and biomechanical properties of native and artificial equine joint cartilage under load using NIR spectroscopy. *Biomed Tech (Berl).* 57: 1059–1061.

91. Afara, I., Sahama, T., and Oloyed, E. A. (2013) Near infrared for non-destructive testing of articular cartilage. In *Nondestructive testing of materials and structures*, Buyukozturk, O., Tasdemir, M. A., Gunes, O., and Akkaya, Y., Eds., Springer Netherlands, Dordrecht, pp. 399–404.

92. Spahn, G., Felmet, G., and Hofmann, G. O. (2013) Traumatic and degenerative cartilage lesions: Arthroscopic differentiation using near-infrared spectroscopy (NIRS). *Arch Orthop Trauma Surg.* 133(7): 997–1002.

93. Padalkar, M. V., Spencer, R. G., and Pleshko, N. (2013) Near infrared spectroscopic evaluation of water in hyaline cartilage. *Ann Biomed Eng.* 41(11): 2426–2436.

94. Guenther, D., Liu, C., Horstmann, H., Krettek, C., Jagodzinski, M., and Haasper, C. (2014) Near-infrared spectroscopy correlates with established histological scores in a miniature pig model of cartilage regeneration. *Open Orthop J.* 8: 93–99.

95. McGoverin, C. M., Lewis, K., Yang, X., Bostrom, M. P. G., and Pleshko, N. (2014) The contribution of bone and cartilage to the near-infrared spectrum of osteochondral tissue. *Appl Spectrosc.* 68(10): 1168–1175.

96. Palukuru, U. P., McGoverin, C. M., and Pleshko, N. (2014) Assessment of hyaline cartilage matrix composition using near infrared spectroscopy. *Matrix Biol.* 38: 3–11.

97. Afara, I. O., Prasadam, I., Moody, H., Crawford, R., Xiao, Y., and Oloyede, A. (2014) Near infrared spectroscopy for rapid determination of Mankin score components: A potential tool for quantitative characterization of articular cartilage at surgery. *Arthroscopy* 30(9): 1146–1155.

98. Afara, I. O., Mood, Y. H., Singh, S., Prasadam, I., and Oloyede, A. (2015) Spatial mapping of proteoglycan content in articular cartilage using near-infrared (NIR) spectroscopy. *Biomed Opt Express.* 6(1): 144–154.

99. Padalkar, M. V., and Pleshko, N. (2015) Wavelength-dependent penetration depth of near infrared radiation into cartilage. *Analyst* 140(7): 2093–2100.

100. McGoverin, C. M., Hanifi, A., Palukuru, U. P., Yousefi, F., Glenn, P. B. M., Shockley, M., Spencer, R. G., and Pleshko, N. (2016) Non-destructive assessment of engineered cartilage composition by near infrared spectroscopy. *Ann Biomed Eng.* 44(3): 680–692.

101. Palukuru, U. P., Hanifi, A., McGoverin, C. M., Devlin, S., Lelkes, P. I., and Pleshko, N. (2016) Near infrared spectroscopic imaging assessment of cartilage composition: Validation with mid infrared imaging spectroscopy. *Anal Chim Acta.* 926: 79–87.

102. Sarin, J. K., Amissah, M., Brommer, H., Argüelles, D., Töyräs, J., and Afara, I. O. (2016) Near infrared spectroscopic mapping of functional properties of equine articular cartilage. *Ann Biomed Eng.* 44(11): 3335–3345.

103. Afara, I. O., Singh, S., Moody, H., Zhang, L., and Oloyede, A. (2016) Characterization of articular cartilage recovery and its correlation with optical response in the near-infrared spectral range. *Cartilage.*

104. Windham, W. R., Lawrence, K. C., and Feldner, P. W. (2003) Prediction of fat content in poultry meat by near-infrared transmission analysis1. *J Appl Poult Res.* 12(1): 69–73.

105. Samuel, D., Park, B., Sohn, M., and Wicker, L. (2011) Visible-near-infrared spectroscopy to predict water-holding capacity in normal and pale broiler breast meat. *Poult Sci.* 90(4): 914–921.

106. Barbin, D. F., Kaminishikawahara, C. M., Soares, A. L., Mizubuti, I. Y., Grespan, M., Shimokomaki, M., and Hirooka, E. Y. (2015) Prediction of chicken quality attributes by near infrared spectroscopy. *Food Chem.* 168: 554–560.

107. Ding, H., Xu, R.-J., and Chan, D.K. (1999) Identification of broiler chicken meat using a visible/near-infrared spectroscopic technique. *J Sci Food Agric.* 79(11): 1382–1388.

108. Jurgens, A., de Mooij, J.D., Logtenberg, H., and Verkleij, T.J. (2005) *Physico-chemical characteristics of ground meat relevant for patty forming and end product quality.* In *Proceedings of the XVII European Symposium on the Quality of Meat and XI European Symposium on the Quality of Eggs and Egg Products*, European Federation of the World's Poultry Science Association, Ed., Doorwerth, Netherlands, 23–26 May 2005, pp. 151–158.

109. Brittberg, M., and Winalski, C. S (2003) Evaluation of cartilage injuries and repair. *J Bone Joint Surg Am.* 85(Suppl. 2): 58–69.

110. Spahn, G., Klinger, H. M., and Hofman, N. G. O. (2009) How valid is the arthroscopic diagnosis of cartilage lesions? Results of an opinion survey among highly experienced arthroscopic surgeons. *Arch Orthop Trauma Surg.* 129(8): 1117–1121.

111. Robert, H., Lambotte, J. C., and Flicoteaux, R. (2011) Arthroscopic measurement of cartilage lesions of the knee condyle: Principles and experimental validation of a new method. *Cartilage* 2 (3): 237–245.
112. Brown, C. P., Jayadev, C., Glyn-Jones, S., Carr, A. J., Murray, D. W., Price, A. J., and Gill, H. S. (2011) Characterization of early stage cartilage degradation using diffuse reflectance near infra-red spectroscopy. *Phys Med Biol.* 56(7): 2299–2307.
113. Luck, W. A. P. (1976) Structure of water and aqueous solutions. *Phys Bl.* 32(7): 334.
114. Ressler, N., Ziauddin, V. C., Janzen, W., and Karachorlu, K. (1976) Improved technics for the near infrared study of water binding by globular proteins and intact tissues. *Society for Applied Spectroscopy* 30(3): 295–302.
115. Sordillo, L. A., Pu, Y., Pratavieira, S., Budansky, Y., and Alfano, R. R. (2014) Deep optical imaging of tissue using the second and third near-infrared spectral windows. *J Biomed Opt.* 19(5): 056004.
116. Geladi, P., MacDougall, D., and Martens, H. (1985) Linearization and scatter-correction for near-infrared reflectance spectra of meat. *Society for Applied Spectroscopy* 39(3): 491–500.
117. Brown, C. P., and Chen, M. (2016) A constituent-based preprocessing approach for characterising cartilage using NIR absorbance measurements. *Biomed Phys Eng Express.* 2(1): 017002.
118. Brown, C. D., Vega-Montoto, L., and Wentzell, P. D. (2000) Derivative preprocessing and optimal corrections for baseline drift in multivariate calibration. *Society for Applied Spectroscopy* 54 (7): 1055–1068.
119. Devaux, M. F., Bertrand, D., Robert, P., and Qannari, M. (1988) Application of principal component analysis on NIR spectral collection after elimination of interference by a least-squares procedure. *Society for Applied Spectroscopy* 42(6): 1020–1023.
120. Tøgersen, G., Arnesen, J. F., Nilsen, B. N., and Hildrum, K. I. (2003) On-line prediction of chemical composition of semi-frozen ground beef by non-invasive NIR spectroscopy. *Meat Sci.* 63(4): 515–523.
121. Wold, S., Sjöström, M., and Eriksson, L. (2001) PLS-regression: a basic tool of chemometrics. *Chemom Intell Lab Syst.* 58(2): 109–130.
122. Bjørsvik, H.-R., and Martens, H. (1998) Data analysis: PLS calibration of NIR instruments by PLS regression. In *Handbook of near-infrared analysis, practical spectroscopy*, Burns, D. A., Ciurczak, E. W., Eds., Taylor and Francis, Boca Raton, FL, pp. 189–205.
123. Heigl, N., Wahl, P., Scheibelhofer, O., Koller, D., Schlingmann, M., Reiter, F., and Straka, G. (2011) NIR spectroscopy with multivariate statistical process control for selected pharmaceutical processes. Paper presented at the Annual Meeting of AIchE, Minneapolis, MN, 16–21 Oct.
124. McGarigal, K., Stafford, S., and Cushman, S. (2000) Discriminant analysis. In *Multivariate statistics for wildlife and ecology research.* Springer: NY, New York, pp. 129–187.
125. Huang, J., Zhao, G., and Dou, W. (2011) [Development of the soft independent modelling of class analogies model to discrimination Vibrio parahemolyticus by Smartongue]. *Wei Sheng Wu Xue Bao.* 51(4): 538–546.
126. Aroen, A. (2004) Articular cartilage lesions in 993 consecutive knee arthroscopies. *Am J Sports Med.* 32(1): 211–215.
127. Curl, W. W., Krome, J., Gordon, E. S., Rushing, J., Smith, B. P., and Poehling, G. G. (1997) Cartilage injuries: A review of 31,516 knee arthroscopies. *Arthroscopy* 13: 456–460.
128. Hjelle, K., Solheim, E., Strand, T., Muri, R., and Brittberg, M. (2002) Articular cartilage defects in 1,000 knee arthroscopies. *Arthroscopy* 18(7): 730–734.